

Envelope Extraction of Underwater Acoustic Echo Using Wavelet and Hilbert Transforms

Chun-xue Shi, Zhi-jin Zhou, Hai-ming Zhao and Mu-rong Zhou

Abstract—To overcome the limitation of the Hilbert transform, this paper proposes a method to extract an envelope of underwater acoustic echoes that uses the wavelet and Hilbert transforms. First, the Hilbert transform is used to extract the envelopes and the wavelet transform is applied to denoise them. A mathematical model of the entire method is established in the process. Second, a test bed for an underwater experiment featuring a data processing system, the acquisition of the echo signal, and feature extraction are described. Finally, underwater acoustic experiments are carried out, and the results show that the proposed approach can extract the echo envelope accurately and can efficiently eliminate interference from random noise. The influence of different wavelet mother functions, the threshold value, and threshold denoising functions is also discussed.

Index Terms—wavelet transform, Hilbert transform, envelope extraction, underwater acoustic echo

I. INTRODUCTION

Research has shown that the shape of an echo from an ultrasonic pulse incident on the seabed is related to the roughness of the bottom of the ocean, the attenuation coefficient of acoustic waves in the sediment, the velocity of sound, and the structure of the density of the seabed. These factors convey information concerning the structure and the physical properties relevant to the sediment [1, 2]. However, the shape of the echo is reflected in that of the amplitude of its envelope to a large extent. The shapes of the amplitudes of envelopes of echoes from sediments with different levels

Manuscript received February 8, 2018; revised March 23, 2020. This work was supported in part by the Chinese National Natural Science Fund Project under Grants 51374245 and 51174087, and the Hunan Natural Science Province and City Unit Fund Project under Grant 2017JJ4038.

Chun-xue Shi is with the Department of Mechanical and Electrical Engineering, Changsha University, Changsha, Hunan, 410003, China (corresponding author, phone: 86-139-75803773; fax: 86-0731-84261492; e-mail: shi_chunxue@163.com).

Zhi-jin Zhou is with the Department of Mechanical and Electrical Engineering, Guizhou Institute of Technology, Guiyang, Guizhou 550003 China (e-mail: zjzhou@hnust.edu.cn).

Hai-ming Zhao is with the Department of Mechanical and Electrical Engineering, Center South University, Changsha, Hunan, 410083, China (e-mail: zhm0097@126.com).

Mu-rong Zhou is with the Department of Mechanical and Electrical Engineering, Center South University, Changsha, Hunan, 410083, China (e-mail: 382634046@qq.com).

of hardness and roughness vary significantly. The amplitude of the envelope of the echo of hard sediment is narrow and sharp, and its peak value is large. The amplitude of the envelope of the echo of soft sediment is flat, but its tail is long. Therefore, features for effective sediment classification can be extracted from this amplitude, including the cumulative energy of the first and second amplitudes of the envelope [3], parameters of hardness and roughness extracted from the envelope of the first echo [4], and the number of fractal dimensions of the envelope [5]. Therefore, the accurate extraction of the amplitude of the envelope of the echo is important for the accurate extraction of features for classification. Because the ultrasonic echo has the narrow-band property [6-7], the amplitude of its envelope can be extracted by the Hilbert transform. However, due to interference from random noise, the Hilbert transformation method generates a rough burr. This paper combines the Hilbert transform with the wavelet transform to overcome the shortcomings of the former and effectively improve the accuracy of envelope extraction.

II. ENVELOPE EXTRACTION BY HILBERT TRANSFORMATION

Assume that $x(t)$ is an acoustic echo signal defined as:

$$\hat{x}(t) = x(t) * \frac{1}{\pi t} = \frac{1}{\pi} \int_{-\infty}^{\infty} \frac{x(\tau)}{t - \tau} d\tau \quad (1)$$

We establish an analytic signal by using $x(t)$ as its real part and $\hat{x}(t)$ as the imaginary part:

$$z(t) = x(t) + j\hat{x}(t) \quad (2)$$

Then, the module of the analytic signal $z(t)$ is called the envelope of the original signal $x(t)$, namely:

$$E(t) = \sqrt{|x(t)|^2 + |\hat{x}(t)|^2} \quad (3)$$

This is the process of extracting the signal envelope by using the Hilbert transform.

The essence of the Hilbert transform is to filter out the component of the negative frequency of $x(t)$ and maintain the phase. Therefore, the Hilbert transform is used to extract the envelope of the signal as well as its high-frequency components. It is susceptible to the influence of random noise and the envelope shows rough burrs. For the underwater acoustic echo signal (the DC component having been removed) shown in Fig. 1, the Hilbert transform is

used to extract the envelope. The result is shown in Fig. 2, where the outline of the extracted envelope is very rough and the influence of random noise is large [9-10], which is not conducive to extracting features for classification.

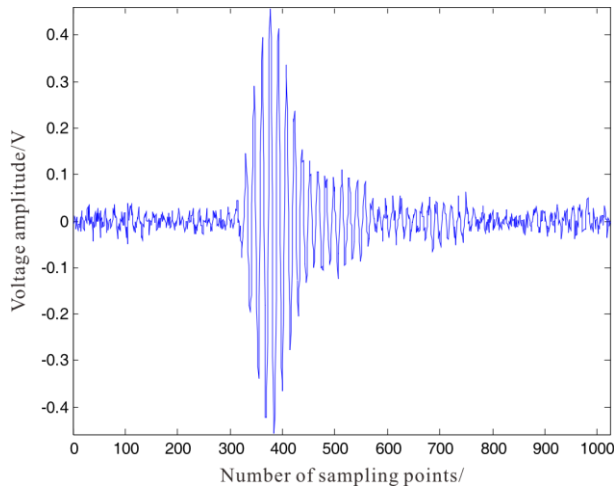


Fig. 1. A measured acoustic echo

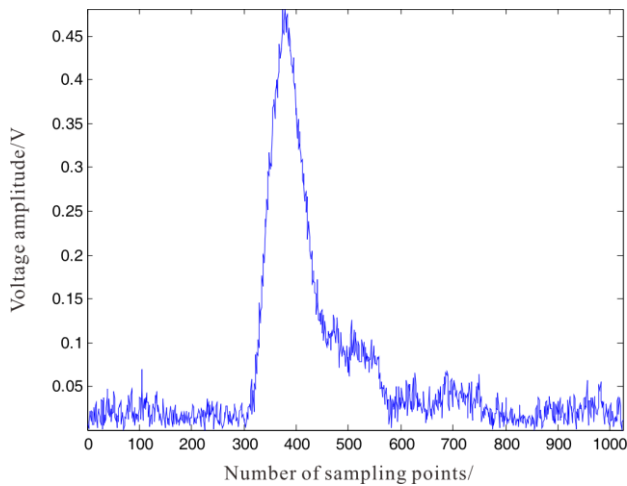


Fig. 2. Envelope extracted by Hilbert-Huang transform

III. DENOISING BY WAVELET TRANSFORMATION

Wavelet analysis can implement multi-resolution time-frequency domain analysis by focusing on any detail of the given signal because of the features of multi-resolution analysis. It has been successfully applied to many fields. In signal processing, wavelet denoising has been applied widely. Many wavelet denoising algorithms are commonly used, of which the threshold method of the non-linear wavelet transform has been widely used because it can obtain the approximate optimal estimation of the original signal, is quick to calculate, and is widely adaptable. Its denoising principle is as follows:

A one-dimensional (1D) signal model with white Gaussian noise can be expressed as follows:

$$s(k) = f(k) + \varepsilon e(k), k = 0, 1, \dots, n-1 \quad (4)$$

where $s(k)$ is the noise signal, $f(k)$ is the useful signal, $e(k)$ is white Gaussian noise, and ε is the noise level. $e(k)$ can be considered as standard white Gaussian noise

that obeys normal distribution $N(0, \sigma^2)$. It is expressed as a high-frequency signal, but in practical engineering, $f(k)$ is generally a low-frequency signal or a relatively stable signal. For the multiple-level decomposition of the wavelet transform, noise signals are generally included in detail with a relatively high frequency. Therefore, the wavelet coefficient can be disposed of by forms, such as the threshold value, and denoising can be implemented by reconstructing the signal [11, 12].

It can be concluded from the above statements that the threshold denoising method of the non-linear wavelet transform can be divided into the following three steps:

- (1) Wavelet decomposition of signals. Select a wavelet, determine its level of decomposition, and use the Mallat algorithm for decomposition calculation.
- (2) Threshold quantization of high-frequency coefficients in wavelet decomposition. In general, noise signals are mostly contained in the details of higher frequencies, because of which a threshold value can be selected to quantify high-frequency coefficients at each scale of decomposition.
- (3) 1D wavelet reconstruction. According to the low-frequency coefficients of the bottom layer and high-frequency coefficients of each layer of wavelet decomposition, 1D wavelet reconstruction is carried out.

IV. ENVELOPE EXTRACTION BY COMBINING THE HILBERT TRANSFORMATION WITH WAVELET ANALYSIS

By using the benefits of the non-linear wavelet transform threshold method to remove noise, and by combining it with the Hilbert transform, an accurate method for extracting the amplitude of the envelope of underwater acoustic echo signals can be obtained. The steps are as follows:

- (1) The original signal is transformed by the Hilbert transform and the envelope of the signal is obtained.
- (2) The wavelet transform of an envelope is implemented.
- (3) The high-frequency coefficients of the wavelet decomposition are quantized by a threshold.
- (4) One-dimensional wavelet reconstruction is used to obtain the envelope of the signal to improve accuracy.

From the above steps, it is clear that the quality of the envelope extracted by the improved method is closely related to the selected orthogonal wavelet bases, scale of wavelet decomposition, threshold, and the threshold quantization processing function.

A. Selecting orthogonal wavelet base

The chosen orthogonal wavelet bases should have high-order vanishing moments. If the vanishing moment is of a low order, singular points in the original signal cannot

be detected. After threshold processing, the singular characteristics of the original signal at these points are weakened, resulting in a large distortion of the signal after noise removal [13]. The selected scale of wavelet decomposition should be relatively large so that noise can be removed to the greatest extent. In general, the maximum theoretical scales of wavelet decomposition can be determined by the following formula:

$$J = \log_2 N - 1 \quad (5)$$

where N is the signal length. The actual maximum scale of wavelet decomposition was slightly smaller than that calculated by the above formula, and can be obtained by the function `wmaxlev(N,'wname')` in the wavelet toolbox of MATLAB.

B. Selecting the threshold value

If the threshold is too low, the signal loses too many details; if the threshold is too high, more details are retained than is necessary and the noise removal is not clean, which reduces the effect of denoising. Usually, the threshold is a fixed value. However, according to the characteristics of noise in the wavelet transform, with an increasing scale of decomposition, the amplitude of the wavelet coefficients of white noise decreases gradually. Therefore, it is unreasonable in theory to quantify different scales with a fixed threshold. The threshold should decrease with the increase in scale [14]. Therefore, it is important to dynamically select the appropriate threshold, the size of which can be determined by the following formula:

$$T_i = \frac{\sigma_i \cdot \sqrt{2 \log N}}{\ln(e + i - 1)} \quad (6)$$

where N is the signal length, i is the corresponding scale of wavelet decomposition of a certain layer ($1 \leq i \leq J$, and J is the maximal scale of wavelet decomposition confirmed in step (1)), and σ_i is the estimated standard difference in the all-level high-frequency coefficient. It can be obtained by dividing the absolute mid-value deviation of the high-frequency coefficient by 0.6745:

$$\sigma_i = \text{median}(\text{abs}(S_i)) / 0.6745 \quad (7)$$

C. Selecting the threshold processing method

Commonly used threshold processing methods include the hard threshold method, soft threshold method, soft-and-hard threshold compromise method, the modular square threshold method, and the bivariate threshold method [15-23].

The soft-and-hard threshold compromise method is as follows:

$$\hat{F}_i = \begin{cases} \text{sign}(S_i)(|S_i| - \alpha T_i) & |S_i| \geq T_i \\ 0 & |S_i| < T_i \end{cases} \quad (8)$$

where $0 \leq \alpha \leq 1$. When $\alpha = 0$, it is the hard threshold value method; when $\alpha = 1$, it is the soft threshold value method.

The modular square threshold method is as follows:

$$\hat{F}_i = \begin{cases} \text{sign}(S_i)(\sqrt{|S_i|^2 - T_i^2}) & |S_i| \geq T_i \\ 0 & |S_i| < T_i \end{cases} \quad (9)$$

The bivariate threshold method is as follows:

$$\hat{F}_i = \begin{cases} S_i \frac{|S_i|^m - T_i^m}{|S_i|^m} & |S_i| \geq T_i \\ 0 & |S_i| \leq \lambda \\ S_i - T_i + \frac{2T_i}{1 + e^{\frac{2S_i}{T_i}}} & \lambda < |S_i| < T_i \end{cases} \quad (10)$$

where $1 < m < +\infty$ and $0 < \lambda < T_i$.

In Formulae (5), (6), and (7), \hat{F}_i is the result of threshold processing, S_i is the i -th high-frequency coefficient of wavelet decomposition, and T_i is the dimension of the threshold value. In the hard threshold value method, because the threshold value function is discontinuous in the selected threshold value, the wavelet coefficients obtained cause oscillation when reconstructing the signal. The soft threshold method filters out all useful signals with periodicity as noise and loses some regularly fluctuating signals. The value adjustment for parameters α , λ , and m in the soft-and-hard threshold value compromise method and bivariate variable threshold value method is a problem. Nevertheless, the effect of the processing of the module square threshold value method combines the advantages of the hard and soft threshold value methods, and thus is used.

From the above analysis, it is clear that the improved method uses the wavelet denoising algorithm to denoise the envelope extracted by the Hilbert transform. Therefore, the differences in the envelope extracted by different wavelet bases, threshold values, and threshold processing functions can be measured using the signal-to-noise ratio (SNR) and the root mean square error (RMSE).

$$RMSE = \sqrt{\frac{1}{n} \sum_{k=1}^n [s(k) - \hat{s}(k)]^2} \quad (11)$$

$$SNR = 10 \log \left(\frac{\sum_{k=1}^n s(k)}{\sum_{k=1}^n [s(k) - \hat{s}(k)]^2} \right) \quad (12)$$

where $s(k)$ is the envelope extracted by the Hilbert transformation and $\hat{s}(k)$ is what was obtained by the proposed method in this paper. If a relatively large SNR and a relatively small RMSE can be obtained by the envelope extracted, this shows that the effect of the proposed method is better.

V. INTRODUCTION TO TEST SYSTEM

A. Pool testbed

A 2,000 mm × 1,600 mm × 1,800 mm rectangular pool was built using the Deep Sea Technology and Equipment Lab of the Center South University with a horizontal undersurface. A guiderail with a stroke of 1,800 mm was installed along the pool's edge. An operational gear with idler wheels was able to walk along the edge to change the detection position. The span of the trolley was 1,600 mm. A fixed device was installed on the ultrasonic transducer in the middle of the trolley platform to be kept below the middle of the trolley. The pool testbed is shown in Fig. 3.



Fig. 3. Pool testbed

B. Data acquisition system

The underwater acoustic signal acquisition system consisted of an ultrasonic transducer, radiating circuit, echo-receiving circuit, master control circuit, and an industrial personal computer. An integrated ultrasonic transducer for underwater transmission and reception developed by the Wuxi CSSC Acoustic Research Technology Center was used as the transducer operated under the water. The transducer was composed of piezoelectric ceramics with a resonant frequency of 500 KHz, a probe diameter of 140 mm, and a 3-dB direction angle of 3°. The radiating circuit comprised a signal-producing circuit, power amplifier circuit, and an impedance matching circuit. The echo-receiving circuit consisted of a pre-amplification electric circuit, TGC circuit (Time Gain Control Circuit), band-pass filtering circuit,

PCI-1714 high-speed acquisition card, and a computer. The master control circuit was the SCM system with the AT89C52 as its core, and was used to complete the generation of the ultrasonic pulse signal, the synchronous trigger of the PCI-1714 high-speed acquisition card, and to adjust the gain in the TGC circuit. The overall structure of the acquisition system for the underwater acoustic signal is shown in Fig. 4.

The process of operation of the system was as follows: the signal acquisition command of the computer was sent through the signal acquisition software once the system had been charged. Then, the SCM AT89C52 started the 555 oscillating circuit to generate 500 KHz of the square signal. The PCI-1714 was started for sampling. The transducer was stimulated to transmit ultrasonic waves once four cycles of the square signal had been subjected to power amplification. The SCM was used to adjust the magnification of the TGC circuit according to time to guarantee that the echo signals were sufficiently amplified. The incident signals of the ultrasonic wave were reflected back after touching an object and received by the ultrasonic transducer. The PCI-1714 carried out the A/D conversion of the echo signals once they had been subjected to pre-amplification, the TGC circuit, and analog band-pass filtering. Then, echo signal data were stored in the computer. The internal control program of the SCM prepared the master control circuit for the next emission following the signal acquisition. The control subprogram of the SCM was programmed in assembly language and the computer data acquisition program was developed in VC++.

C. Echo signal acquisition

The waveform of a certain sampled signal is shown in Fig. 6. A total of 20,000 sampling points included both the transmitted signal and the true echo signal of the sediment.

The waveform before the 2,000th point was the incident signal and the waveform around the 16,000th point was the echo signal. The echo signal of all 20,000 points and the incident signals were subject to cross-correlation in order to find the starting point of the true echo. A total of 1,024 points were intercepted at the starting point of the echo as the true echo, and were sufficient for containing the true echo through several experimental observations. A sample was randomly extracted from 160 true echo signal sets for each kind of sediment. The waveform of a sampled signal is shown in Fig.5.

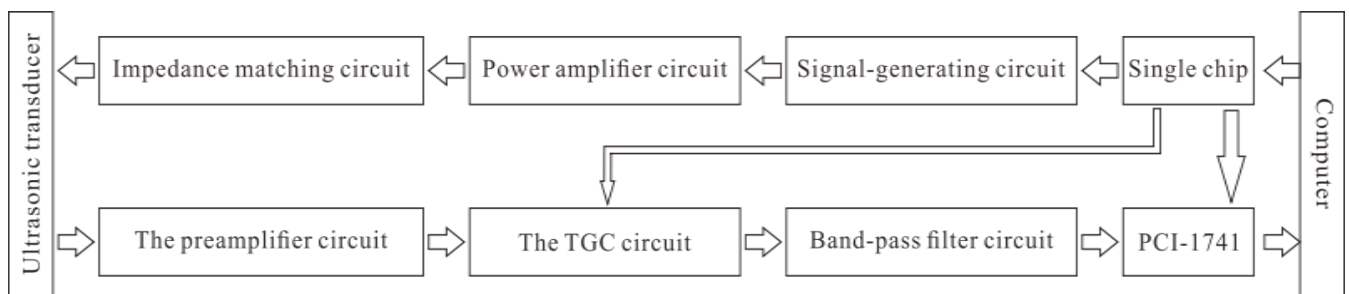


Fig. 4. Structural composition of the signal acquisition system

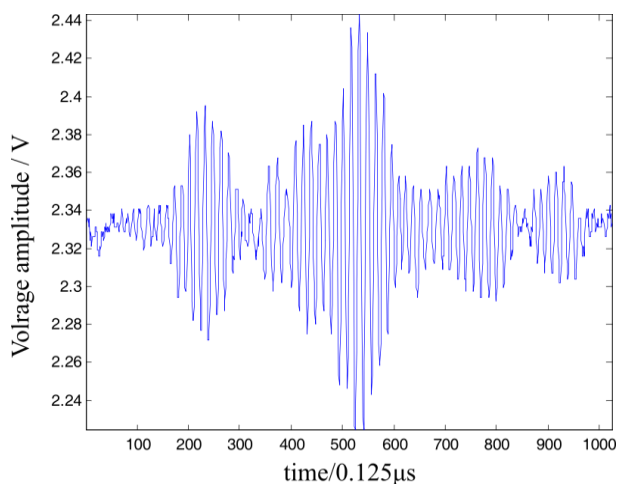


Fig. 5. Waveform of a sampled signal

D. Extracting features of generalized dimensions

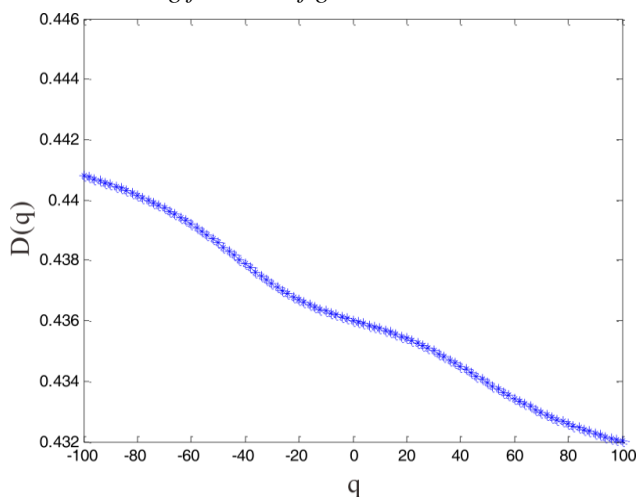


Fig. 6. One kind of generalized dimension spectrum

The procedure for calculating the generalized dimensions was used to extract features of the generalized dimension for the collected echo signals of the sediments. The range of values of q was $[-100,100]$ at intervals of two. The result is shown in Fig. 6.

VI. EXPERIMENTAL ANALYSIS

To verify the effectiveness of the proposed envelope extraction method, the small wave basis Coif5 was selected, with a maximal decomposition scale of five and a dynamic threshold value set according to Formula (6).

Envelope extraction was implemented on the original underwater acoustic echo signal shown in Fig. 1 according to the method proposed in this paper, as shown in Fig. 7 (the blue line shows the amplitude if the envelope is extracted by

adopting the Hilbert transformation, and the red line shows the envelope extracted by the proposed method). It is clear that the proposed method obtained a better effect.

To further analyze and compare the advantages and disadvantages of the wavelet basis, the threshold value, and the threshold processing method in the envelope extraction, the original underwater acoustic echo signal in Fig. 1 was extracted using the method proposed in this paper. The results are shown in Fig. 8, and the performance evaluation parameters were compared as shown in Tables 1 and 2.

Table 1 compares the effects of envelope extraction at different threshold values and with threshold processing methods when the wavelet bases were Db8.

Table 2 compares the effects of the envelope extraction of different wavelet bases when the same threshold values and threshold processing methods were used.

TABLE 1

COMPARISON OF DIFFERENT THRESHOLD VALUES AND THRESHOLD PROCESSING METHODS WITH THE SAME WAVELET

Evaluation parameter	Hard threshold method and dynamic threshold value	Soft threshold method and dynamic threshold value	Module square threshold method	
			Dynamic threshold value	Fixed threshold value
SNR	19.335	18.370	19.4166	11.5764
RMSE	0.0128	0.0143	0.0127	0.0312

TABLE 2

COMPARISON OF DIFFERENT WAVELETS WITH THE SAME THRESHOLD VALUES AND THRESHOLD PROCESSING METHODS

Evaluation parameter	Db8	Sym8	Coif5
SNR	19.4166	19.3708	19.7235
RMSE	0.0127	0.0129	0.0112

Table 1 shows that the effect of the modular square threshold method was better than that of the hard and soft threshold methods, and the effect of the dynamic threshold method was better than that of the fixed threshold method. As shown in Table 2, Coif5 based on the wavelet delivered the best effect because it had higher-order loss moments, and was superior to the other two wavelets in terms of support length, symmetry, and orthogonality.

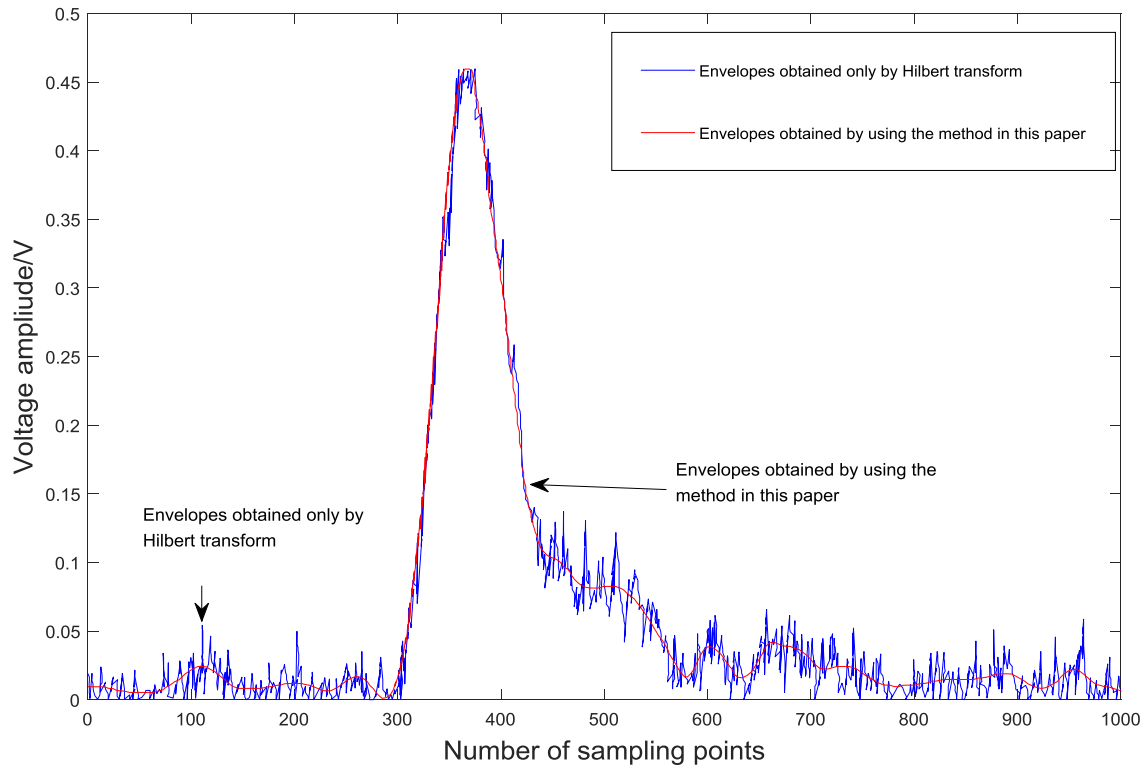


Fig. 7. Comparison between methods of envelope extraction

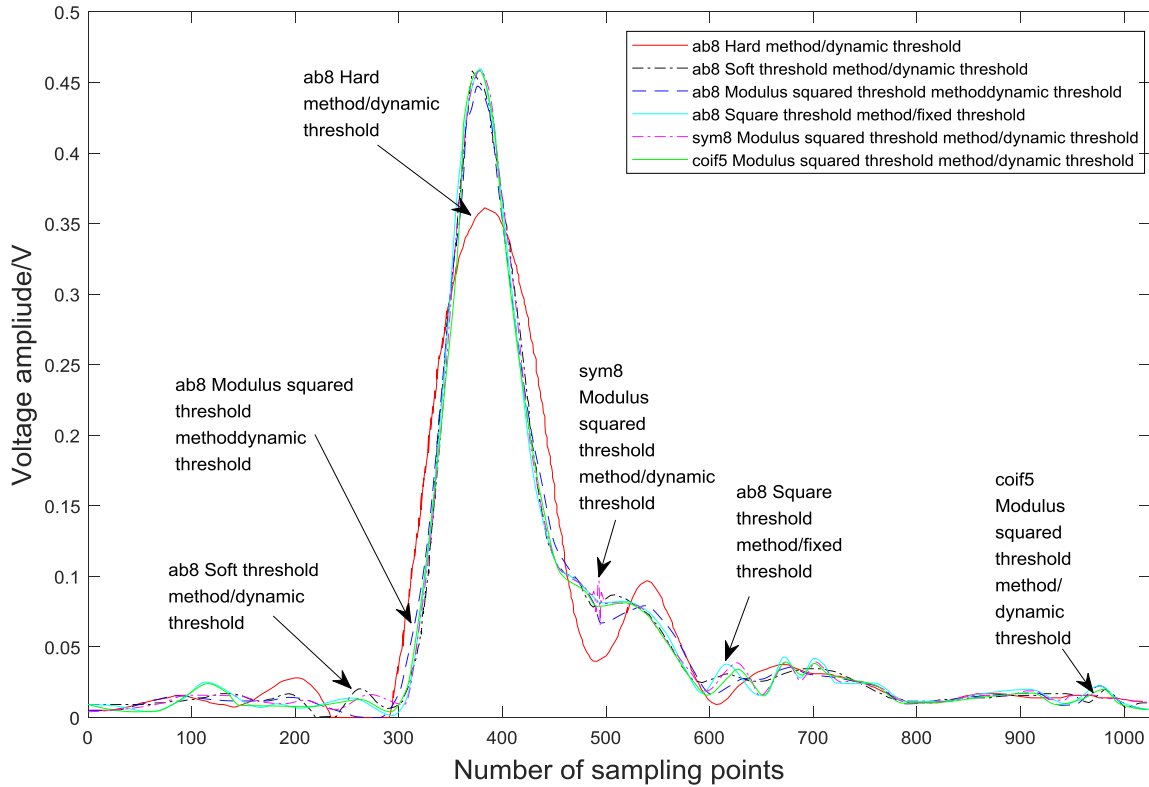


Fig. 8. Comparison of different wavelets, threshold values, and threshold processing methods

VII. CONCLUSION

(1) Due to the interference of random noise, the envelope obtained by the Hilbert transform method produces rough burrs and the obtained envelope is rough.

(2) Using the advantage of the non-linear wavelet transform threshold method in terms of removing noise, and by combining it with the Hilbert transform, a highly precise method was developed to extract the amplitude of the envelope of underwater acoustic echo signals.

(3) Experimental results show that the proposed method can compensate for the shortcomings of the Hilbert transform, obtain clear envelope contours, eliminate the influence of random noise, and significantly improve the quality of the envelope. Moreover, with an appropriate wavelet basis, threshold size, and threshold processing function, its effect can be further improved.

ACKNOWLEDGMENTS

The authors are grateful to the editor and anonymous referees, who helped improved the quality of this paper.

REFERENCES

- [1] J.S. Meng and D.H. Guan, "Acoustical Classification of Sea Floor Sediments," *Acta Acustica*, vol. 7, no. 6, pp. 337-343, 1982.
- [2] H.N. Huang and Z.S. Li, "A New Practical Way for Classifying Lake Bottom Sediment," *Journal of Northwestern Polytechnical University*, vol. 16, no. 3, pp. 421-426, 1998.
- [3] A. ORLOWSKI, "Application of multiple echo energy measurements for evaluation of sea bottom type," *Ocenologia*, vol. 19, no. 3, pp. 61-78, 1998.
- [4] D. BAKIERA and A. STEPNOWSKI, "Method of the sea bottom classification with a division of the first echo signal," *Proceedings of the XIIIth Symposium on Hydroacoustics*, Gdynia-Jurata, pp. 55-60, 1996.
- [5] P. BARAT and S. BANDYOPADHYAY, "Fractal property of backscattered acoustic signals from polycrystalline aluminium," *Physics Letters A*, vol. 245, pp. 91-96, 1988.
- [6] Z.J. Zhou, Z.J. Wen and Y.Y. Bu, "Application study of wavelet analysis on ultrasonic echo wave noise reduction," *Chinese Journal of Scientific Instrument*, vol. 30, no. 2, pp. 237-241, 1998.
- [7] H.K. Jiang, D.D. Dou and Z.J. He, "A New Method for Identifying Ultrasonic Echo Signal Features Using Adaptive Second Generation Wavelet," *Journal of North western Poly technical University*, vol. 29, no. 1, pp. 93-96, 2011.
- [8] H.Y. Zhang, Q. Zhou and J.D. Xia, "Wavelet Packet Denoising and Feature Extract ion for Flaw Echo Signalin Ultrasonic Testing," *Chinese Journal of Scientific Instrument*, vol. 27, no. 1, pp. 94-98, 2006.
- [9] L. Wen, Z.S. Liu and Y.J. Ge, "Several methods of wavelet denoising," *JOURNAL OF HEFE IUNIVERSITY OF TECHNOLOGY*, vol. 25, no. 2, pp.167-172, 2006.
- [10] L. Wen, Z.S. Liu and E.W. Chen, "Correlation Wavelet Method for Structural System Identification," *China Mechanical Engineering*, vol. 17, no.5, pp.449-452, 2006.
- [11] J.G. Zhan, Y. Wang and H.Z. Xu, "The Wavelet Analysis of Sea Level Change in China Sea during 1992 ~ 2006," *ACTA GEODAETICA et CARTOGRAPHICA SINICA*, vol. 37, no. 4, pp.438-443, 2008.
- [12] Z.B. Xu, J.P. Xuan and T.L. Shi, "Identification of modal parameters using crosscorrelation technique and wavelet transform," *Huazhong Univ. of Sci. & Tech. (Natural Science Edition)*, vol. 36, no. 5, pp.67-70, 2008.
- [13] G.Y. Tu, L.P. Yang and J.J. Cui, "Study on an Approach of Signal Noise Separation Based Wavelet," *JOU RNAL OF NATIONAL UNIVERSITY OF DEFENSE TECHNOLOGY*, vol. 21, no. 4, pp.40-43, 1999.
- [14] H.Y. Wen, "Research on Deformation Analysis Model Based upon Wavelet Trans form Theory," *ACTA GEODAETICA et CARTOGRAPHICA SINICA*, vol. 34, no. 2, pp.186-187, 2005.
- [15] L. DONOHO and I. JOHNSTONE, "Ideal spatial adaptation by wavelet shrinkage," *Biometrika*, vol. 81, no. 3, pp.425-455, 1994.
- [16] X.X. Liu, Q.G. Wei and S.T. Wang, "Identification of Marine Oil Spills by Fisher Discriminant Based on Discrete Wavelet Transform," *Spectroscopy and Spectral Analysis*, vol. 37, no. 11, pp.3479-3484, 2017.
- [17] J.D. Wang and W.J. Pan, "Application of Fisher discriminant analysis in steady-state power quality evaluation of grid-connected photovoltaic system," *Electric Power Automation Equipment*, vol. 37, no. 3, pp.50-54, 2017.
- [18] J.C. Guo, F. Zhang and N. Wang, "Image Classification Based on Fisher Constraint and Dictionary Pair," *Journal of electronics and information technology*, vol. 39, no. 2, pp.270-277, 2017.
- [19] Z.H. Zhao and L. Chen, "A Context-Aware Recommendation Method with Multi-Feature Fusion Based on Fisher Linear Discriminant Analysis," *Journal of Xi'an Jiaotong University*, vol. 51, no. 8, pp.40-46, 2017.
- [20] M.X. Xue, S.R. Liu and J.A. Wang, "Dynamic Multi-Target Recognition Based on Machine Vision," *Journal of Shanghai Jiaotong University*, vol. 51, no. 6, pp.727-733, 2017.
- [21] Y.Q.Zeng, H.B.Li, X.Xia and Bo Liu, "Analysis on Time-frequency features and Delay Time Identification for Blasting Vibration Signal by Hilbert-Huang Transform in Fangchenggang Nuclear Power Station," *Engineering Letters*, vol. 25, no. 3, pp.329-335, 2017.
- [22] B.W.Zheng, J.S.Wang and Y.L.Ruan, "Recognition Method Based on Gabor Wavelet Transform and Discrete Cosine Transform," *Engineering Letters*, vol. 26, no. 2, pp.228-235, 2018.
- [23] Z.H.Xia, C.S.Yuan and X.M.Sun, "Combining Wavelet Transform and LBP Related Features for Fingerprint Liveness Detection," *IAENG International Journal of Computer Science*, vol. 43, no. 3, pp.290-298, 2016.

Chun-xue Shi (1980.3-), male, born in Baoding, Hebei province, China. Lecturer, PhD, worked in Changsha, Hunan province, China, Department of Mechanical and Electrical Engineering, Changsha University. The main research direction is the key technology and equipment of seabed mining. Tel: +86-139-75803773, E-mail: shi_chunxue@163.com.